

# CuRTAIL: ChaRacterizing and Thwarting Adversarial deep Learning

Bita Darvish Rouhani, Mohammad Samragh, Tara Javidi, Farinaz Koushanfar

University of California San Diego

bita@ucsd.edu, msamragh@ucsd.edu, tjavidi@ucsd.edu, farinaz@ucsd.edu

**Abstract**—This paper proposes CuRTAIL, a novel end-to-end computing framework for characterizing and thwarting adversarial space in the context of Deep Learning (DL). The framework protects deep neural networks against adversarial samples, which are perturbed inputs carefully crafted by malicious entities to mislead the underlying DL model. The precursor for the proposed methodology is a set of new quantitative metrics to assess the vulnerability of various deep learning architectures to adversarial samples. CuRTAIL formalizes the goal of preventing adversarial samples as a minimization of the space unexplored by the pertinent DL model that is characterized in CuRTAIL vulnerability analysis step. To thwart the adversarial machine learning attack, CuRTAIL introduces the concept of Modular Robust Redundancy (MRR) as a viable solution to achieve the formalized minimization objective. The MRR methodology explicitly characterizes the geometry of the input data and the DL model parameters. It then learns a set of complementary but disjoint models which maximally cover the unexplored subspaces of the target DL model, thus reducing the risk of integrity attacks. We extensively evaluate CuRTAIL performance against the state-of-the-art attack models including fast-sign-gradient, Jacobian Saliency Map Attack, and Deepfool. Proof-of-concept implementations for analyzing various data collections including MNIST, CIFAR10, and ImageNet corroborate CuRTAIL effectiveness to detect adversarial samples in different settings. The computations in each MRR module can be performed independent of the other redundancy modules. As such, CuRTAIL detection algorithm can be completely parallelized among multiple hardware settings to achieve maximum throughput. The execution overhead of each MRR module is the same as that of the main DL model. We further provide an accompanying automated Application Programming Interface (API) to facilitate the adoption of the proposed framework for various applications.

## I. INTRODUCTION

Security and safety consideration is the biggest obstacle for the wide-scale adoption of emerging learning algorithms in sensitive scenarios such as intelligent transportation, health-care, and video surveillance applications [1], [2], [3]. While advanced learning technologies are essential for enabling coordination and interaction among autonomous agents and the environment, a careful analysis of their security as well as thwarting their vulnerabilities is still in its infancy. Machine learning models including the state-of-the-art deep neural networks are widely used in various scientific fields ranging from speech recognition [4], [5] and computer vision [6], [7] to financial fraud [8] and malware detection [9], [10]. These applications have been mainly developed with an implicit security assumption about the generalizability of such models for evaluation of unseen examples. Recent results on adversarial

machine learning, however, have shed light on a new and largely unexplored surface for malicious attacks jeopardizing the reliability of machine learning models [11], [12], [13].

As shown in several recent studies, a malicious adversary can carefully manipulate the input data by leveraging specific vulnerabilities of learning techniques to undermine the integrity of a certain system [1]. Misclassifying a certain source class into a distinct target class is one of the strongest adversarial goals for attackers targeting classifiers as outlined in [13], [14], [15]. The problem of adversarial samples arises due to the fact that machine learning algorithms are designed for stationary environments where the training and test data are collected from the same unknown distributions. This working hypothesis, however, can be easily violated by adversaries to mislead the learning system.

A vast majority of recent research efforts have focused on devising new attack methodologies in particular for the popular class of deep learning algorithms with limited attention to possible countermeasures [11], [12], [13]. The existing research works which have considered viable countermeasures for adversarial deep learning can be categorized into three classes: (i) Denoising encoders have been suggested in the literature as a pre-processing step to improve the robustness of DL networks by mapping the adversarial samples into the original input space. As shown in [16], however, the resulting two-stage DL network is no more difficult to attack than the original one. (ii) Several recent papers have focused on training the DL model by including adversarial examples in the training set [17], [12], [18], [19]. Although this technique has yielded significant improvement in the convergence of the underlying model and robustness to particular noise patterns in the input space, it can only partially evade adversarial samples from being effective as shown in [20]. (iii) Distillation is another countermeasure recently proposed in [21]. This technique aims to improve the robustness of DL networks by transforming the original model into a second model that lies in a smoother gradient space compared to the original one. However, recent follow-up papers (e.g., [22]) have demonstrated that the distilled network is as vulnerable to adversarial attacks as the original network.

This paper proposes CuRTAIL, a holistic framework for characterizing and thwarting adversarial deep learning space. CuRTAIL formalizes the goal of preventing adversarial samples as an optimization problem to minimize the unexplored space in the target DL model. To fulfill this objective, we introduce a new defense mechanism called Modular Robust

Redundancy (MRR). MRR approach is motivated by our key observation that no single model can completely eliminate the potential adversarial space by relying on a limited set of labeled data. As such, instead of using a single module for detection of adversarial samples, CuRTAIL employs multiple minimally overlapping *redundant modules (defender models)* that investigate each input sample in parallel to the main DL model and raise alarm flags for those samples that are suspected to be infected. Compared to the existing DL defense mechanisms (e.g., [16], [21], [12]), our proposed approach is beneficial due to three main reasons: (i) Existing works either restrict the accuracy of the main DL model or particularly rely on altering the current DL topologies and/or training process to make the model more robust against adversarial samples. In CuRTAIL neither the training complexity nor the final accuracy of the main DL model is affected. (ii) In order to adjust the level of security in most of the existing works, the victim DL model should be retrained with alternative hyper-parameters, whereas in CuRTAIL the hardness of the detection policy can be easily adjusted once a defender model has been trained. (iii) The use of parallel redundancy modules in CuRTAIL framework significantly reduces the risk of integrity attacks as the attacker requires to simultaneously deceive all the defender models to succeed.

For a given DL model (victim network), CURTAIL first evaluates the relative vulnerability of each layer based on the spectral analysis of the DL parameters. It then learns a set of disjoint redundancy modules to maximally cover the vulnerable space in the target application while constraining the number of redundancy modules. The redundancy modules in CuRTAIL framework are built upon the commonly-used dictionary learning method [23]. Each dictionary targets a certain layer in the neural network. For each layer, the corresponding dictionary explicitly characterizes the statistical properties of input data and DL parameters by learning the pertinent probability density function (PDF) of the latent variables. Finally, the learned dictionaries are utilized to analyze the features in the input and intermediate layers of the DL model and identify potential adversarial samples.

The security level in CuRTAIL is quantified by a high-level parameter that can be adjusted to account for various application-specific requirements. We empirically and analytically investigate the security of CuRTAIL framework as a viable countermeasure for adversarial deep learning. We consider a white-box attack model in which the attacker knows everything about the victim (DL network) including its model topology, learning algorithm, and parameters. This threat model represents the most powerful attacker that can endanger the real-world machine learning applications. An accompanying CuRTAIL API is provided to ensure its ease of use for deployment of DL applications including several computer vision tasks, malware detection, and biometric recognition. CuRTAIL API is devised with an automated customization unit to adjust the number of modular redundancies in accordance with a set of user-defined constraints such as real-time data analysis prerequisites and pertinent security requirements. Note that the

redundancy modules can be parallelized on different hardware to achieve maximum throughput.

The explicit contributions of this paper are as follows:

- Proposing CuRTAIL, a novel end-to-end framework for characterizing and thwarting adversarial space in the context of deep learning. We incept the idea of Modular Robust Redundancy as a viable security countermeasure for adversarial machine learning. For a fixed number of redundancy modules, CuRTAIL carefully learns a set of complementary dictionaries to maximally cover the unexplored space in the victim DL model and effectively reduce the risk of integrity attacks.
- Providing quantitative measurements to characterize the sensitivity of DL model layers from the statistical point of view. This is crucial since the number of MRR modules can be limited in several real-world settings. We utilize the formalized sensitivity measurement to optimally identify DL layers for which MRR modules should be established.
- Performing extensive evaluations on well-known DL applications including MNIST [24], CIFAR10 [25], and ImageNet [26] benchmarks. The results demonstrate the algorithmic practicality and system performance efficiency of CuRTAIL framework against state-of-the-art attack models including fast-sign-gradient [12], Jacobian Saliency Map attack [13], and Deepfool [27].
- Implementing an automated accompanying API to facilitate adoption/integration of the proposed framework for the reliable realization of different DL applications. CuRTAIL incorporates high-level security parameters into the proposed defense mechanism, allowing users to effectively adjust the robustness of the countermeasure without requiring them to get involved in the details of the design.

## II. BACKGROUND AND PRELIMINARIES

A machine learning model refers to a function  $f$  and its associated parameters  $\theta$  that are particularly trained to infer/discover the relationship between input samples  $x \in \{x_1, x_2, \dots, x_N\}$  and the expected labels  $y \in \{y_1, y_2, \dots, y_N\}$ . Each output observation  $y_i$  can be either continuous as in most regression tasks or discrete as in classification applications. Machine learning algorithms typically aim to find the optimal parameter set  $\theta$  such that a loss function  $\mathcal{L}$  that captures the difference between the output inference and ground-truth labeled data is minimized:

$$\theta = \underset{\theta}{\operatorname{argmin}} \frac{1}{N} \sum_{i=1}^N \mathcal{L}(f(x_i, \theta), y_i). \quad (1)$$

In this paper, we focus our evaluations on the state-of-the-art deep learning models due to their popularity in the realization of various autonomous learning systems. Consistent with the literature in this field, we particularly centralize our discussions on the classification tasks using DL methodology. However, we emphasize that the core concept proposed in this paper is rather more generic and can be used for reliable deployment of different learning techniques such as generalized

linear models, regression methods (e.g., regularized regression (Lasso)), and kernel support vector machines.

### A. Deep Learning

Deep learning is an important class of machine learning algorithms that has provided a paradigm shift in our ability to comprehend raw data by showing superb inference accuracy resembling the learning capability of human brain [2], [3]. A DL network is a hierarchical learning topology consisting of several processing layers stacked on top of one another. The schematic depiction of a typical DL network consisting of convolutional, pooling, fully-connected, and various non-linearity layers is demonstrated in Figure 1. This type of neural networks is widely adopted in computer vision and image processing tasks [6]. Table I summarizes common layers used in DL neural networks. The state of each neuron (unit) in a DL network is determined in response to the states of the units in the prior layer after applying a nonlinear activation function. In Table I,  $x_i^{(l)}$  is the state of unit  $i$  in layer  $l$ ,  $z_i^{(l)}$  is the post-nonlinearity value associated with unit  $i$  in layer  $l$ ,  $\theta_{ij}^{(l)}$  specifies the parameter connecting unit  $j$  in layer  $l$  and unit  $i$  in the layer  $l + 1$ , and  $k$  indicates the kernel size used in 2-dimensional (2D) layers.

TABLE I: Commonly used layers in DL neural networks.

DL Layers		Description
<b>Core Computations</b>	<b>Fully-Connected</b>	$x_i^{(l)} = \sum_{j=1}^{N_{l-1}} \theta_{ij}^{(l-1)} \times z_j^{(l-1)}$
	<b>2D Convolution</b>	$x_{ij}^{(l)} = \sum_{s_1=1}^k \sum_{s_2=1}^k \theta_{s_1 s_2}^{(l-1)} \times z_{(i+s_1)(j+s_2)}^{(l-1)}$
<b>Normalization</b>	<b><math>L_2</math> Normalization</b>	$x_i^{(l)} = \frac{x_i^{(l)}}{\sqrt{\sum_{j=1}^{N_l}  x_j^{(l)} ^2}}$
	<b>Batch Normalization</b>	$x_i^{(l)} = \frac{x_i^{(l)} - \mu_B^{(l)}}{\sqrt{\frac{1}{b_s} \sum_{j=1}^{b_s} (x_j^{(l)} - \mu_B^{(l)})^2}}$
<b>Pooling</b>	<b>2D Max Pooling</b>	$x_{ij}^{(l)} = \text{Max}(y_{(i+s_1)(j+s_2)}^{(l-1)}) \quad \begin{matrix} s_1 \in \{1, 2, \dots, k\} \\ s_2 \in \{1, 2, \dots, k\} \end{matrix}$
	<b>2D Mean Pooling</b>	$x_{ij}^{(l)} = \text{Mean}(z_{(i+s_1)(j+s_2)}^{(l-1)}) \quad \begin{matrix} s_1 \in \{1, 2, \dots, k\} \\ s_2 \in \{1, 2, \dots, k\} \end{matrix}$
<b>Non-linearities</b>	<b>Softmax</b>	$z_i^{(l)} = \frac{e^{x_i^{(l)}}}{\sum_{j=1}^{N_l} e^{x_j^{(l)}}}$
	<b>Sigmoid</b>	$z_i^{(l)} = \frac{1}{1 + e^{-x_i^{(l)}}}$
	<b>Tangent Hyperbolic</b>	$z_i^{(l)} = \frac{\text{Sinh}(x_i^{(l)})}{\text{Cosh}(x_i^{(l)})}$
	<b>Rectified Linear unit</b>	$z_i^{(l)} = \text{Max}(0, x_i^{(l)})$

Training a DL network involves two main steps: (i) forward propagation, and (ii) backward propagation. These steps are iteratively performed for multiple rounds using different batches of known input/output pairs  $(x_i, y_i)$  to reach a certain level of accuracy. In forward propagation, the raw values of the input data measurements are gradually mapped to higher-level abstractions based on the current state of the DL parameters ( $\theta$ ). The acquired data abstractions are used to predict the inference label in the last layer of the DL network based on a Softmax regression.<sup>1</sup> In backward propagation, an optimization algorithm such as stochastic gradient descent [28]

<sup>1</sup>Softmax regression (or multinomial logistic regression) is a generalization of logistic regression that maps a  $P$ -dimensional vector of arbitrary real values to a  $P$ -dimensional vector of real values in the range of  $[0, 1]$ . The final inference for each input sample can be determined by the output unit that has the largest conditional probability value.

is performed to find the gradient direction along which the DL parameter set  $\theta$  should be updated to minimize the distance between network prediction (output of forward propagation) and the ground-truth label.

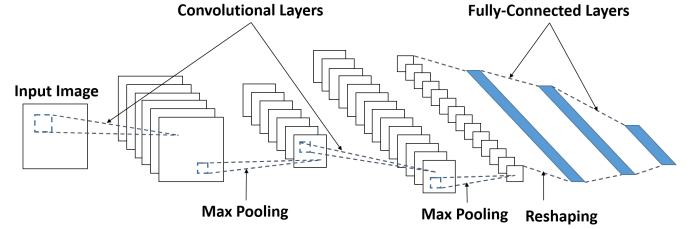


Fig. 1: Schematic depiction of a typical neural network used for computer vision and image processing tasks.

Once the DL network is trained to deliver a desired level of accuracy, the model is employed as a classification oracle in the execution phase (a.k.a., test phase). During the execution phase, the model parameters  $\theta$  are fixed and prediction is performed through one round of forward propagation for each unknown input sample. Attacks based on adversarial samples target the execution phase of DL networks and do not involve any tampering with the training procedure as will be discussed in Section III.

### III. ATTACK MODELS

Adversarial machine learning can be cast as a zero-sum Stackelberg game between the machine learning oracle (victim) and the attacker. Depending on the attacker's knowledge, the threat model can be categorized into three classes:

- **White-box attack.** The attacker knows everything about the defender model including the learning algorithm, model topology, and parameters, but has limited or partial access to the training data [12], [12], [13].
- **Gray-box attack.** The attacker only knows the underlying learning algorithm and model topology but has no access to the training data or the trained parameters.
- **Black-box attack.** The attacker knows nothing about the pertinent machine learning algorithm, model, or training data. This attacker only can obtain the corresponding inference label for input samples. In this setting, the adversary can perform a differential attack by observing the output changes with respect to the input variations [29].

A complete taxonomy of adversarial capabilities and goals are provided in [13], [14], [15]. In this paper, we consider the white-box threat model as the most powerful attacker that can appear in real-world machine learning applications.

In an adversarial setting, the attacker aims to find a perturbed adversarial sample  $(x^a)$  such that it incurs minimal distance from the source sample  $(x^s)$  while its corresponding output is sufficiently different to mislead the victim. Figure 2 illustrates an example, where the image on the left is initially classified correctly as a dog by the victim model while adding a small amount of perturbation to the original image has misled the victim to infer it as a black swan (right image).

Clearly, if the source instance is already misclassified by the victim model ( $f(x^s, \theta) \neq y^*$ ), the adversarial problem becomes trivial. Therefore, we particularly focus on instances  $x^s$  that could have been classified correctly by the oracle before adding structured adversarial noises ( $f(x^s, \theta) = y^*$ ).

We define the distance between the machine learning oracle output and the ground-truth label as follows:

$$\mathcal{D}(f(x^a), y^*) = \gamma_0 \mathcal{L}(f(x^a), y^*) - \sum_{f(x^a) \neq y^*} \gamma_i \mathcal{L}(f(x^a), y_i), \quad (2)$$

where  $\mathcal{L}$  is the loss function used to train the pertinent DL model,  $\gamma_0 \geq 0$  is the weight for the ground-truth and  $\gamma_i \geq 0$  are the weights for each misleading target. Hence, the adversarial objective is to find the solution to the following:

$$\operatorname{argmax}_{x^a} \mathcal{D}(f(x^a), y^*) \text{ s.t. } \|(x^a - x^s)\|_\infty \leq \epsilon. \quad (3)$$

To solve for the optimal adversarial sample ( $x^a$ ), the adversary should compute the sensitivity of each DL output with respect to the changes in the input features. The network sensitivity can be computed in several ways. Figure 3 depicts the schematic depiction of adversarial attacks. Below we briefly describe state-of-the-art attack mechanisms against which we evaluate CuRTAIL. Details about each attack algorithm can be found in the corresponding paper.



Fig. 2: An example of (a) source input data, and (b) its corresponding adversarial sample. The added noise is visually hard to see but makes the victim misclassify (b).

**Fast Sign Gradient (FSG).** Authors in [12] suggested the *fast-sign-gradient* method that leverages the sign of the loss function's gradient with respect to each input feature to craft the adversarial samples. In this case, the adversarial sample per input feature ( $x_i^a$ ) is computed as:

$$x_i^a = x_i^s + \epsilon \operatorname{sign}\left(\frac{\partial \mathcal{L}}{\partial x_i^s}\right), \quad (4)$$

which guarantees that the overall perturbation ( $\|(x_i^a - x_i^s)\|_\infty$ ) does not exceed the threshold  $\epsilon$ . The computed gradient in fast-sign-gradient is similar to the cost evaluated in back-propagation step in the training phase with a key difference that the derivative is computed with respect to the input features ( $x_i^s$ ). Parameter  $\epsilon$  determines the closeness of the crafted adversarial sample to the legitimate input. Higher  $\epsilon$  values result in higher attack success rate with the cost of more distinguishable additive noise.

**Jacobian Saliency Map Attack (JSMA).** A different attack methodology was recently introduced in which the network sensitivity per input feature is computed by applying the Jacobian gradient of the DL output to the source input. In

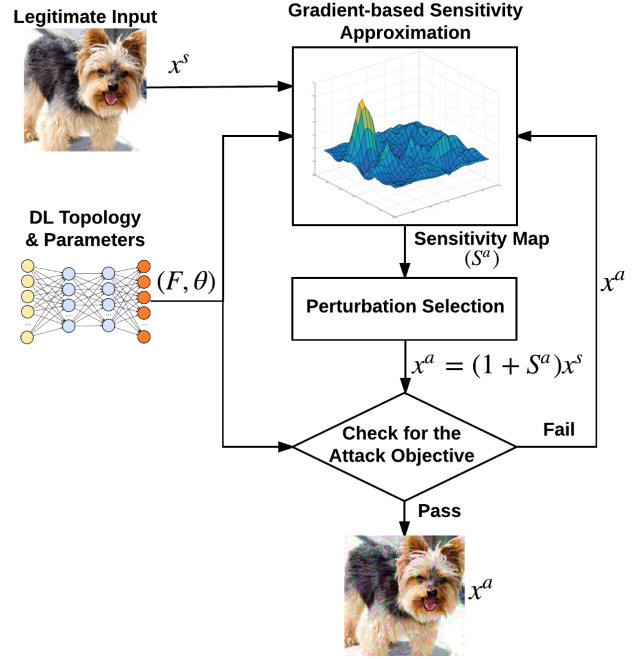


Fig. 3: Overall flow of the adversarial attack methodologies as suggested in [12], [13], [27].

particular, authors in [13] suggested computing the sensitivity map per input feature ( $x_i^s$ ) as:

$$x_i^a = x_i^s + \begin{cases} 0 & \text{if } \frac{\partial f_t(x^s)}{\partial x_i^s} < 0 \text{ or } \sum_{j \neq t} \frac{\partial f_j(x^s)}{\partial x_i^s} > 0 \\ \frac{\partial f_t(x^s)}{\partial x_i^s} \left| \sum_{j \neq t} \frac{\partial f_j(x^s)}{\partial x_i^s} \right| & \text{otherwise} \end{cases}, \quad (5)$$

where  $t$  indicates the desired target class towards which the adversary wants to mislead the classifier,  $x_i$  is the  $i^{\text{th}}$  element (pixel) in the input, and  $f_j$  is the probability of the  $j^{\text{th}}$  class in the output Softmax layer. As opposed to the FSG attack, this attack is an iterative algorithm that changes one pixel in a single iteration. In each iteration, the pixel with the highest value in the saliency map is chosen and increased by  $\epsilon$  (assuming that pixels can take a value between 0 and 1). Updated pixels are also clipped to remain in the valid range. Compared to the FSG approach, the JSMA attack adds a smaller amount of perturbation to the input data but it usually achieves a lower success rate (i.e., it can generate fewer adversarial samples). In this paper, we characterize the JSMA attack using two parameters: (i)  $\epsilon$  which determines the maximum perturbation added to each pixel, and (ii)  $n_{\text{iters}}$  denoting the maximum number of pixels updated.

**Deepfool.** Authors in [27] have introduced another attack heuristic called Deepfool that carefully adds perturbations to minimize the  $L_2$  distance of the adversarial sample and the original data. Deepfool is also an iterative algorithm where in each iteration all pixels are modified based on a certain update rule. We refer the reader to the original paper for further explanation of the attack algorithm. We characterize the Deepfool attack using two parameters throughout this paper:  $\epsilon$  which determines a constant multiplied by the update noise

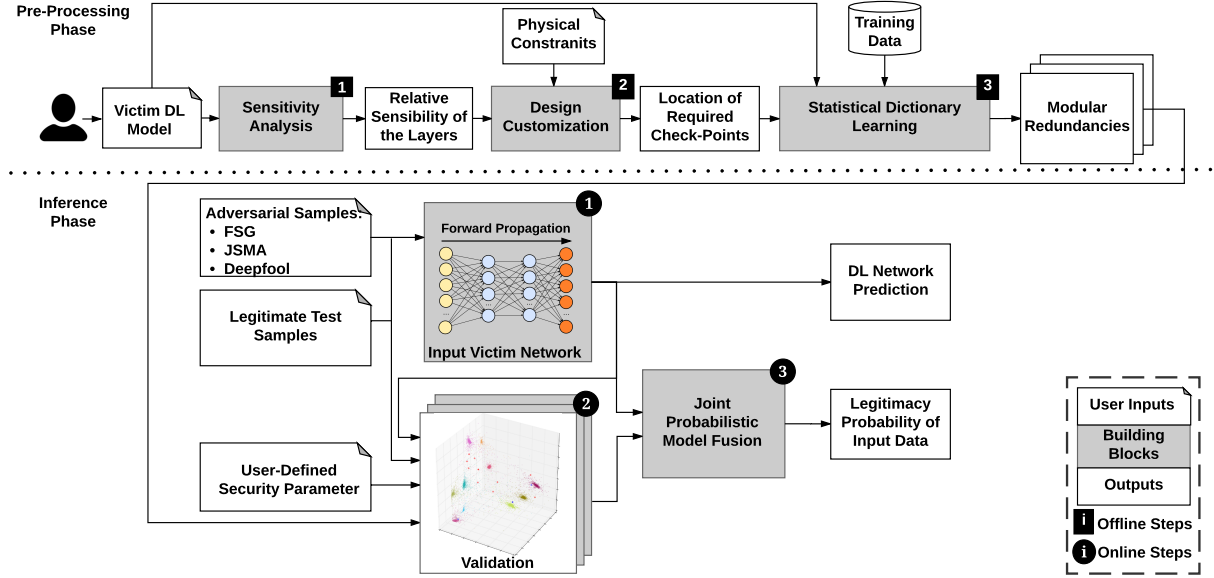


Fig. 4: Global flow of CuRTAIL framework including both off-line (pre-processing) and online (inference) phases. The pre-processing phase includes analyzing the vulnerability of the input neural network (called victim) and learning a set of redundancy modules (defensive dictionaries) to maximally cover the unexplored space in the victim model. The learned dictionaries are used in the inference phase to detect potential adversarial samples fed into the victim DL network.

vector in each iteration, and  $n_{iters}$  that denotes the maximum number of iterations to craft adversarial samples.

#### IV. CURTAIL GLOBAL FLOW

Figure 4 illustrates the global flow of CuRTAIL framework. CuRTAIL consists of two main phases to analyze the vulnerability of a victim DL model and detect the adversarial samples that might be fed into the underlying network.

**(i) Pre-Processing Phase.** The pre-processing phase is performed in three successive steps.

**1 Sensitivity Analysis.** CuRTAIL framework takes a trained DL neural network as its input and primarily performs a thorough sensitivity analysis based on a layer-wise spectrum density evaluation of pertinent model parameters (Section V-A). This information is leveraged to find the vulnerable space of the DL model to the potential adversarial samples and identify the layers in the neural network for which the modular redundancies should be learned.

**2 Design Customization.** There is a trade-off between the execution runtime and the system reliability in terms of successful detection rate (Section V-D). CuRTAIL takes user-defined physical constraints such as real-time requirements into account and determines the viable number of redundancy modules (checkpoints) and their appropriate locations based on the sensitivity of DL layers computed in step 1.

**3 Statistical Dictionary Learning.** The key building block of CuRTAIL framework is the dictionary learning unit in which a set of redundancy modules (checkpoints) are learned based on statistical properties of the training data and the victim model parameters (Section V-B). To do so, CuRTAIL first

trains a set of complementary neural networks (defenders) with the goal of separating data manifolds in each checkpointing layer by careful realignment of legitimate training data within each class (Section V-B1). The complementary networks pose an exact structure of the victim model. The key difference between the defenders and the victim model is the loss function for which each of these models is optimized. Once the complementary neural networks are trained, CuRTAIL uses the probability density function of the acquired features to learn the corresponding dictionary of each checkpoint location.

Note that the pre-processing phase in CuRTAIL framework is an off-line process that is only performed once per DL application. The cost of CuRTAIL pre-processing is amortized over time as the DL network and its associated defensive redundancy modules are employed for online DL inference.

**(ii) Inference Phase.** In the inference phase, the incoming adversarial samples (Section III) along with the legitimate test data are simultaneously fed to the victim and defender models. CuRTAIL goes through three steps to find the inference label for each incoming data and provides a precise confidence interval for the network prediction.

**1 Forward Propagation.** The predicted class for each incoming sample is acquired through forward propagation in the main DL network (victim model). CuRTAIL defense mechanism is devised to provide a confidence interval for the network prediction. This confidence interval is used for validation of the input-output pairs in the target application and does not impact the accuracy of the main model.

**2 Validation.** CuRTAIL leverages the statistical dictionaries learned in the previous steps to validate the legitimacy of

the input data and the associated output. In particular, samples that do not lie in the *user-defined* probability interval which we refer to as the *Security Parameter (SP)* are discarded as suspicious samples. SP is a constant number in the range of [0 – 100] that determines the hardness of adversarial detectors. For applications with excessive security requirements, a high SP value should be set to assure full detection of adversarial samples. A high detection rate (e.g., 100%) may come at the cost of having several false positives in the detection process as will be discussed in Section VI.

**3 Joint Probabilistic Model Fusion.** The outputs of the redundancy modules (dictionaries) are finally aggregated to compute the legitimacy probability of the input data and its associated inference label (Section V-C).

## V. CURTAIL METHODOLOGY

The existence of adversarial samples indicates the presence of small (in the Euclidean distance sense) additive noise patterns in the input space that can make a large impact on the model’s output. This phenomenon particularly happens due to two main reasons:

**(i) Linear behavior in high-dimensional spaces.** Small amounts of perturbation in the input space are exacerbated by successive projections through different layers of a DL network. Mathematically speaking, for each input sample  $x$ , the output of a DL network consisting of  $L$  successive layers is computed as follows:

$$f(X, \theta) = f_L(f_{L-1}(\dots f_1(x, \theta_1), \theta_2), \dots, \theta_L) \quad (6)$$

where  $f_l$  is the mapping operator used in layer  $l$  and  $\theta_l$  is the corresponding parameter set of that layer. As such, the overall instability of the DL system is the multiplication aggregate of the instability of each layer [11]. In other words,

$$S = \prod_{l=1}^L S_l, \quad (7)$$

where  $S_l$  indicates the instability of layer  $l$ . In Section V-A, we provide quantitative measures to characterize the instability of each layer normalized to the possible perturbation levels.

**(ii) Insufficient regularization in supervised learning.** A machine learning model built upon a limited set of labeled data is strongly-robust against adversarial samples if and only if it is trained based on an exact subset of features used by the perfect oracle (e.g., human annotator) [30]. Although DL networks with a more complex topology (e.g., a network with a deeper structure and more number of neurons per layer) can potentially achieve a better accuracy, they are also more vulnerable to adversarial attacks due to the larger space unexplored by such models. Our hypothesis is that a proper feature representation learning is the key to obtain a learning model that is both accurate and robust. As we discuss in Section V-B, adversarial samples can be effectively detected by careful checkpointing in the intermediate stages based on probabilistic dictionaries learned from the data and DL parameter distributions.

### A. Spectral Analysis of DL Sensitivity

The perturbation signal in adversarial samples can be cast as an additive noise added to the input data. In particular, for each layer  $F_l$  we define the instability as:

$$\text{Sup}_{r \neq 0} \frac{\|f_l(x_l + r_l) - f_l(x_l)\|}{\|r_l\|}, \quad (8)$$

where  $\text{Sup}$  stands for the supremum value,  $x_l$  is the input to the  $l^{\text{th}}$  layer, and  $r_l$  is the additive perturbation propagated to the input of that layer. For instance, for a fully-connected layer with parameter set  $\theta_l$ , Eq. (8) is equivalent to:

$$\text{Sup}_{r \neq 0} \frac{\|f_l(x_l + r_l) - f_l(x_l)\|}{\|r_l\|} = \frac{\|\theta_l \times r_l\|}{\|r_l\|} \leq \|\theta_l\|, \quad (9)$$

where the last step is obtained by applying the Cauchy-Schwarz inequality. The same equation applies to convolutional layers for which the Tensor kernels should be vectorized to form  $\theta_l$ .

The instability of core computation layers (e.g., fully-connected and convolution layers) is bounded by the spectrum of their underlying parameters. Considering the principal spectrum of the parameter set  $\theta_l$ , the upper bound in Equation (9) is achieved if and only if the perturbation vector  $r$  is aligned with the main Eigenvector of the underlying parameters. To quantify and compare the instability of various layers in a DL network, we suggest using the *Spectral Energy Factor (SEF)* preserved by the first Eigenvalue as a measurement to identify most sensitive intermediate layers. The SEF metric is computed as:

$$\text{SEF}(\theta_l) = \frac{|e_1|}{\sum_{i=1}^{\min(N_{l-1}, N_l)} |e_i|}, \quad (10)$$

where  $|e_i|$  is the absolute value of the  $i^{\text{th}}$  Eigenvalue and  $N_l$  is the number of neurons (units) in the layer  $l$ . The sensitivity of specific non-linearity layers outlined in Table I is upper bounded by their Lipschitz constant as shown in [11].

### B. Modular Robust Redundancy

CuRTAIL redundancy modules (checkpoints) are classified into two distinct categories: (i) *Latent dictionaries* that are particularly trained for probabilistic separation of latent features acquired in the intermediate layers of the DL network (Section V-B1). These dictionaries are utilized to approximate the corresponding PDF for each class and identify the atypical samples. (ii) *Input dictionaries* that are learned from the original dataset for each class of data. These dictionaries are used to detect suspicious noise patterns in the input domain (Section V-B2). As we empirically demonstrate in Section VI, adversarial samples are not transferable in between the redundancy modules as each dictionary is learned for a unique objective function. In other words, if an adversarial sample can bypass one of the checkpoints, it will most likely be detected by other redundancy modules.

### 1) CuRTAIL Latent Dictionaries:

To learn statistical properties of latent features, CuRTAIL first trains a set of complementary neural networks (one for each checkpoint corresponding to a certain intermediate layer). Each complementary neural network aims to minimize the Euclidean distance between data samples of the same class while maximizing the same metric for samples of different classes. This goal is achieved through several rounds of iterative realignment of training data at each checkpoint location.

The complementary neural networks (defenders) have an exact structure of the main input DL model. The main difference between the new models and the input DL network is the loss function for which each of these networks is optimized. To learn the distribution of latent variables in a particular layer of the neural network, CuRTAIL first initiates a complementary model with the same topology and parameters. An  $L_2$  normalization layer (Table I) is also inserted in the desired checkpoint location. The normalization layer aims to map the latent feature variables into the Euclidean space such that the acquired data embeddings live on a d-dimensional hyper-sphere, i.e.,  $\|f(x)\|_2 = 1$ . This normalization is crucial as it partially removes the effect of over-fitting to particular data samples that are highly correlated with the pertinent DL parameter set<sup>2</sup>.

Once the defender model is set up, the following term is added to the conventional cross-entropy loss function:

$$\mathcal{L}+ = \gamma [\|C^{y^*} - f(x)\|_2^2 - \Sigma_{i \neq y^*} \|C^i - f(x)\|_2^2], \quad (11)$$

where  $\gamma$  specifies the contribution of the additive term,  $f(x)$  is the intermediate feature vector extracted from sample  $x$ ,  $y^*$  is the true label, and  $C^i$  denotes the center of all features corresponding to class  $i$  as suggested in [31]. Minimizing the overall loss function allows CuRTAIL to fine-tune the complementary network parameters such that the squared distance between data measurements within the same class is small, while the squared distance between a pair of inputs from different classes is large. The center points are a part of DL parameters that are iteratively learned by the complementary network.

Figure 5 illustrates the feature vectors in a checkpoint layer before and after retraining. In this example, we consider the LeNet300-100-10 model [32] trained on a dataset of handwritten digits known as MNIST (the checkpoint is inserted after the hidden layer with 100 units). Each color in Figure 5 indicates a certain category (10 total classes). As shown, the diversity of latent variables within a particular class is minimized while the distances between different classes are magnified after retraining. To avoid unnecessary variations, we use Principal Component Analysis [33] to project feature vectors into a low-dimensional subspace such that more than 99% of energy is preserved. CuRTAIL fits a Gaussian Mixture Model (GMM) to the acquired low dimensional features

<sup>2</sup>The  $L_2$  norm can be easily replaced by an arbitrarily user-defined norm through our accompanying API.

and learns the corresponding dictionaries such that they best represent the data structure in the checkpoint location.

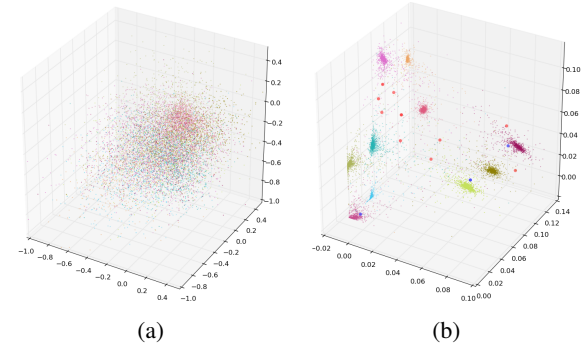


Fig. 5: Example output of a complementary neural network in CuRTAIL framework. (a) Latent feature samples in the main DL model (victim). (b) Latent feature samples of the same layer in the complementary neural network. The big dot points in this figure demonstrate example adversarial inputs. The red dot points can be easily detected as they incur a very low legitimacy probability in CuRTAIL defensive mechanism. The blue dot points can be effectively detected using complementary dictionaries in the input space even with a low SP parameter.

The big dot points in Figure 5 correspond to adversarial samples generated by the fast-sign-gradient attack methodology [12]. The majority of adversarial samples (e.g., the red dot points) reside in space regions with low density of training samples. Therefore, the estimated probability for adversarial samples is significantly smaller than that of legitimate instances. Note that the adversarial samples cannot be differentiated from the legitimate ones in the primary network but they can be identified in the defender network as most of them lie in the low-density regions of the Euclidean space (red dot points in Figure 5). Adversarial samples that live within the high-density region (blue dot points in Figure 5) of GMM are detected in CuRTAIL framework by leveraging dictionary learning input space as will be discussed in Section V-B2. We emphasize that training the defender networks is a one-time process that can be performed off-line.

For each incoming test sample, CuRTAIL first finds the log-likelihood of the pertinent latent features computed for that sample using the statistical latent dictionaries. The acquired log-likelihood is then compared against a threshold obtained from the user-defined security parameter (SP). Figure 6 illustrates how the SP can control the hardness of the decision function. In this example, we have depicted the latent features of one category that are projected into the first two PCA components in the Euclidean space (each dot point corresponds to a single input image). The blue and black contours in Figure 6 correspond to security parameters of 10 and 20, respectively. For example, 10% of the legitimate training samples lie outside the contour specified by  $SP = 10$ . The decision function for distinguishing adversarial and legitimate samples works as follows: any incoming data whose latent features lie within

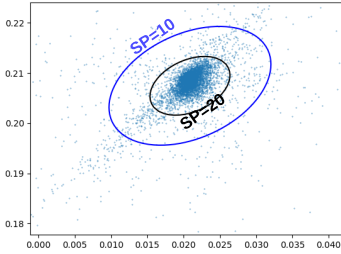


Fig. 6: Illustration of the effect of security parameter (SP) on the detection policy. A high SP leads to a tight boundary which treats most samples as adversarial examples.

the boundary dedicated by the SP is considered a legitimate sample. A higher SP tightens the boundary beyond which samples are inferred as suspicious examples.

## 2) CuRTAIL Input Dictionary:

Many modern data collections are either low-rank or lie on a union of lower dimensional subspaces [34], [35]. To effectively identify adversarial samples, CuRTAIL utilizes compressing sensing and sparse coding algorithms to represent the pertinent features as an ensemble of lower-rank embeddings by learning a set of dictionaries that best represent the training data. Particularly, CuRTAIL learns a separate dictionary for each class by solving:

$$\underset{D^i}{\operatorname{argmin}} \frac{1}{2} \|x^i - D^i v^i\|_2^2 + \alpha \|v^i\|_1 \quad \text{s.t.} \quad \|D_K^i\| = 1, \quad (12)$$

$$0 \leq K \leq K_{max}$$

Here,  $x^i$  is a matrix whose columns are pixels extracted from different regions of input images belonging to category  $i$ . For instance, if we consider  $8 \times 8$  patches of pixels, each column of  $x^i$  would be a vector of 64 elements. The goal of dictionary learning is to find matrix  $D^i$  that best represents the distribution of pixel patches from images belonging to class  $i$ . We denote the number of columns in  $D^i$  by  $K_{max}$ . For a certain  $D^i$ , the image patches  $x^i$  are represented with a sparse matrix  $v^i$ , and  $D^i v^i$  is the reconstructed patch. Therefore, the first term  $\|x^i - D^i v^i\|_2^2$  in the objective function (Equation 12) enforces low reconstruction error. The second term enforces sparsity to matrix  $v^i$ , which is controlled using hyper-parameter  $\alpha$ . As we empirically show in section VI, the sparsity of matrix  $v^i$  enables the input dictionary module to effectively remove added perturbations from adversarial input samples. The dictionary matrix is first initiated with a set of random samples from input data. The dictionary samples are then gradually updated with samples that best represent the data content in each category. Figure 8 illustrates the sample dictionary patches learned for classes 4 and 5 of MNIST dataset. CuRTAIL provides an automated solver to facilitate dictionary learning for data scientists and practitioners.

For each incoming sample, during the execution phase, CuRTAIL takes the output of the main DL model (e.g., class

$i$ ) and denoises the data sample by reconstructing it with the corresponding dictionary  $D^i$ : patches of pixels within an input image are first encoded as a sparse matrix  $v^i$  using the Orthogonal Matching Pursuit (OMP) algorithm [36], which is a well-known routine for solving compressed sensing problems. OMP iteratively approximates the sparse representation  $v^*$  of the input sample  $x^i$  by adding the best fitting dictionary element in each iteration. Suppose the dictionary matrix  $D^i$  contains a set of samples that commonly appear in the training data belonging to class  $i$ , thus the input sample classified as class  $i$  can be reconstructed as  $D^i v^*$ , where  $v^*$  is the optimal solution obtained by OMP with a certain sparsity level.

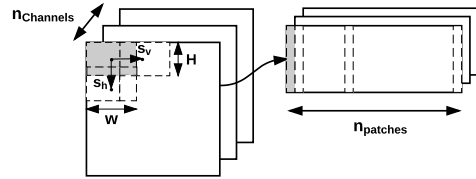


Fig. 7: Image to patch conversion: each input image is mapped to a series of overlapping data patches to be processed in the input dictionary learning. A similar approach can transform the processed data patches back to the input image size.

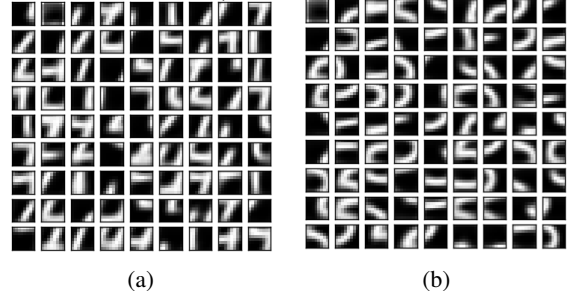


Fig. 8: Example MNIST input dictionary patches for (a) class 4, and (b) class 5. In this experiment, we used a patch size of  $7 \times 7$  with no overlapping.

For input samples in the image and video format, CuRTAIL converts each frame into a series of patches that contain the values of neighboring pixels as illustrated in Figure 7. The size of each data patch and the desired overlap between two successive patches are algorithmic parameters that are tuned with respect to the application data. The input data patches are then used to learn the dictionary samples and reconstruct testing data. The reconstructed patches can be converted back into the initial format for comparison purposes.

Figure 9 illustrates the flow of CuRTAIL input dictionary defensive module. The denoising module automatically detects and removes possible adversarial perturbations from input samples. Once the denoised input sample is constructed, CuRTAIL evaluates the main DL model (i.e., the victim model) on the denoised input. If the predictions for the original and the denoised inputs are not compatible, CuRTAIL raises an alarm flag indicating that the input might be an adversarial sample. The hardness of noise cancellation is determined by

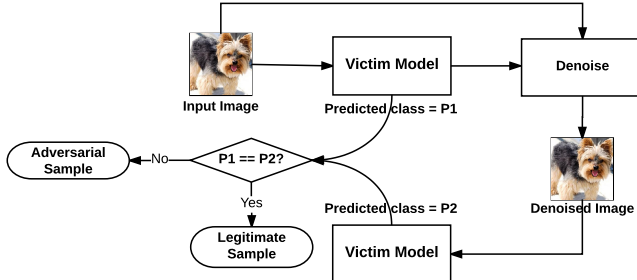


Fig. 9: CuRTAIL detection using input dictionaries.

the number of nonzero elements in the sparse representation  $v^*$ , which can be tuned for different applications. We elaborate on the effect of sparsity on detection accuracy in Section VI.

### C. Joint Probabilistic Model Aggregation

The output of redundancy modules in CuRTAIL framework are combined in a weighted aggregation setting. The weight of each redundancy module can be easily set by users in our provided API to account for prior knowledge about the testing environments of the underlying application. In the default setup of our API, the contribution (weight) of each latent dictionary is set in accordance with the sensitivity of the corresponding DL layer. Let us denote the contribution of the  $i^{th}$  latent dictionary by  $C^i$ . As such,  $C^i$  is primary set to  $SEF(\theta_i)$  where  $SEF(\theta_i)$  is defined in Equation (10). The weights of the latent dictionaries are then scaled such that:

$$\sum_{i=1}^{N_{MRR}} C^i = 1, \quad (13)$$

where  $N_{MRR}$  is the total number of modular redundancies.

The aggregated results of the latent dictionaries for each sample is used along with the output of the input dictionary to determine the legitimacy level of an input-output pair in CuRTAIL framework. In our experiments in Section VI, we assume an equal contribution for the aggregated latent feature dictionaries and the input dictionary.

### D. Complexity and Reliability Trade-off

There is a trade-off between the computational complexity (e.g., runtime overhead) of the modular redundancies and the reliability of the overall system. On the one hand, a high number of validation checkpoints increases the reliability of the systems, but it also increases the computational load as each input sample should be validated by more defender networks. On the other hand, a small number of checkpoints degrades the defense mechanism performance by treating adversarial samples as legitimate ones. The execution complexity of each latent dictionary is equivalent to the cost of one forward propagation in the target model. This is because each complementary network has a similar topology as the victim model. For the input dictionary detector, the complexity of computing the sparse representation for a single patch of pixels is  $\mathcal{O}(m \times K \times K_{max})$ , where  $K_{max}$  is the number of samples in the pertinent dictionary,  $m$  is the number of input features (i.e., pixels in the patch), and  $K$  is the desired number of nonzeros

in the sparse representation. Figure 10 demonstrates the utility and reliability trade-off for analyzing MNIST dataset on LeNet DL model. The runtime is normalized with respect to the cost of one forward propagation in the target neural network. In this experiment, the DL execution is performed *sequentially* on an NVIDIA GeForce 980 GPU hosted by an Intel core-i7 CPU. We emphasize that MRR computations (different colored bars in Figure 10) can be run in parallel to minimize the runtime overhead.

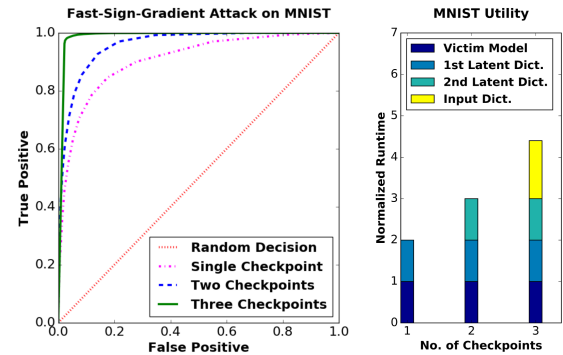


Fig. 10: Complexity and reliability trade-off for analyzing MNIST dataset on LeNet DL model.

CuRTAIL takes the user-defined runtime constraint for DL execution of one sample in the target application as its input. Our framework provides automated subroutines to perform platform profiling on various CPU and CPU-GPU hardware. The platform profiling is a one-time process and takes  $10 - 100$  msec depending on the hardware platform. CuRTAIL adjusts the number of viable checkpoints according to the user-specific runtime constraint and available computational resource provisioning. The intermediate DL layers are prioritized based on the instability analysis outlined in Section V-A. Due to the space limits, we focus our experiments in Section VI on using only two checkpoints, one in the input data space and one in the last hidden layer of the neural network prior to the output layer. This setup corresponds to the minimum overhead for the proposed defense mechanism (twice the execution time in the primary network). As shown in Figure 10, intermediate checkpoints can be used to effectively improve the detection performance in the target application.

## VI. EVALUATIONS

We evaluate CuRTAIL framework on three canonical machine learning datasets: MNIST [24], CIFAR10 [25], and ImageNet [26]. Figure 11 illustrates several representative samples from each dataset.

**MNIST Benchmark.** The MNIST data is a collection of 70000 black and white images of handwritten digits where the goal is to classify the written digits (0–9) into one of the potential 10 classes. The images are normalized such that each pixel takes a real value in the range of 0 to 1. The original data is split into 60000 training samples and 10000 test samples.



Fig. 11: Example legitimate samples in each benchmark dataset. These samples are randomly selected from each of the target classes in the MNIST (top row), CIFAR10 (middle row), and ImageNet (bottom row) datasets.

TABLE II: Baseline (victim) network architectures for evaluated benchmarks. Here, **128C3(2)** denotes a convolutional layer with 128 maps and  $3 \times 3$  filters applied with a stride of 2, **MP3(2)** indicates a max-pooling layer over regions of size  $3 \times 3$  and stride of 2, and **300FC** is a fully-connected layer consisting of 300 neurons. All convolution and fully connected layers (except the last layer) are followed by ReLU activation functions. A Softmax activation function is applied to the last layer of each network.

Benchmark	Architecture
MNIST	$784 - 300FC - 100FC - 10FC$
CIFAR10	$3 \times 32 \times 32 - 300C3(1) - MP2(2) - 300C2(1) - MP2(2) - 300C3(1) - MP2(2) - 300FC - 100FC - 10FC$
Imagenet	$3 \times 224 \times 224 - 96C11(4) - 256C5(1) - MP3(2) - 128C3(1) - MP3(2) - 128C3(1) - 128C3(1) - MP3(2) - 1024FC - 1024FC - 10FC$

In our experiments for this dataset, we train and use the DL topology proposed in [32] which is also available in Table II.

**CIFAR10 Benchmark.** The CIFAR10 data [25] is a collection of 60000 color images of size  $32 \times 32$  that are classified in 10 categories: Airplane, Car, Bird, Cat, Deer, Dog, Frog, Horse, Ship, and Truck. The images are represented in three (red, green, blue) channels and are normalized such that each pixel takes a value in the  $[0 - 1]$  range. We split the data samples into a set of 50000 training data and a set of 10000 test data. In our experiments, we train and use the state-of-the-art DL topology proposed in [37] for the CIFAR10 dataset. Details about the architecture are available in Table II.

**ImageNet Benchmark.** ImageNet [26] is a large database consisting of over 15 million data samples. The images are collected from the web and human-labeled using Amazon’s Mechanical Turk tool. Typically, a subset of images belonging to 1000 different categories is used by the research community for learning evaluation of ImageNet data [6]. In our experiments, we train and use a DL architecture inspired by the well-known AlexNet [6] DL topology for ImageNet classification. Details about the trained model are available in Table II. We down-sample ImageNet classes by a factor of 100 for execution efficiency purposes. The selected classes include Tinca Tinca fish (a.k.a., Tench), black swan, Chrysanthemum dog, tiger beetle, academic gown and robe, cliff dwelling, hook and claw, paper towel, one-armed bandit, and water tower.

TABLE III: Details of training for victim and defender models.

Benchmark	MNIST	CIFAR10	ImageNet
<b>Victim Accuracy</b>	98.4%	80.5%	82.6%
<b># Training Iterations (Victim)</b>	100	300	100
<b># Training Iterations (Defender)</b>	100	300	100

In our evaluations, we leverage momentum and parameter decay to ensure model convergence and utilize the dropout technique [38] to avoid over-fitting. The performance of our DL realization for each benchmark is consistent with the state-of-the-art DL models that have been evaluated on these datasets. Table III presents the accuracy of the victim model and the number of iterative training epochs for the baseline and defender models.

#### A. CuRTAIL Open-Source API

We provide an accompanying end-to-end API to ensure easy adoption of CuRTAIL framework by data scientists and engineers<sup>3</sup>. Our implementations for multi-core CPU and CPU-GPU platforms are built to work with the highly popular DL library known as TensorFlow [39]. CuRTAIL API takes user-specific variables such as DL model and training data, the desired security parameter  $SP$  (which, in turn, defines the hardness of defensive redundancy modules), and the underlying physical constraints in terms of runtime budget for DL execution of one data sample in the target application (Section V-D). The accompanying API automates the sensitivity analysis, design customization, and dictionary learning processes in CuRTAIL framework. The current realization of CuRTAIL framework provides support for DL sensitivity analysis against state-of-the-art attacks including fast-sign-gradient (FSG) [12], Jacobian Saliency Map attack (JSMA) [13], and Deepfool [27]. Our API is implemented based on an object-oriented design. As such, new modular redundancies and/or new attack models can be easily incorporated in our API by simply defining the desired functionality as a new class.

#### B. CuRTAIL Performance Against Adversarial Attacks

To illustrate the effect of our defense algorithm, we create adversarial samples using the three attack scenarios described in Section III. More specifically, we set the parameters of each attack algorithm as outlined in Table IV. When we applied the JSMA attack on the Imagenet dataset, the success rate was low and the algorithm was slow. To address this issue, we modified the original algorithm as follows: instead of changing only one pixel in each iteration, we jointly modified the top-100 pixels with highest values in the corresponding saliency map. This approach significantly improved the attack success rate for high-resolution images of Imagenet. To ensure the effectiveness of our defense mechanism against smallest perturbations, we empirically evaluated the quality of the crafted adversarial samples and insured that the additive perturbations are quite small. As detailed in Table IV, the average mean squared error is fairly small (maximum of 1.85e-3), making the detection

<sup>3</sup>Codes are available at <https://github.com/Bitadr/CuRTAIL>

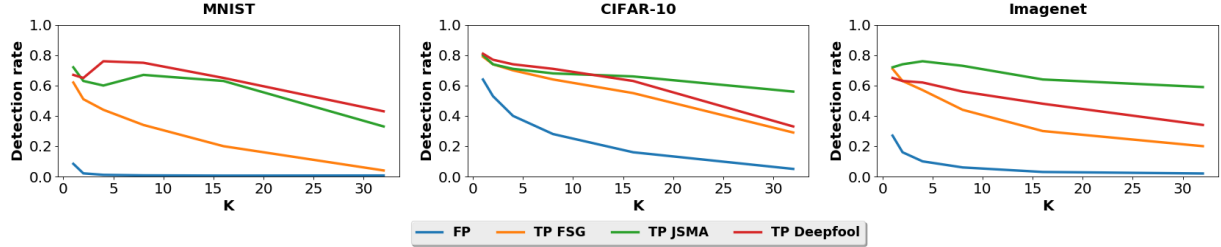


Fig. 12: Evaluation of CuRTAIL input denoising module for different number of non-zeros  $K$  for the OMP algorithm. False Positive (FP) and True Positive (TP) rates decrease as  $K$  increases. TP-FSG, TP-JSMA, and TP-Deepfool denote the detection rates corresponding to the three attack algorithms.

TABLE IV: Details of attack algorithms and mean-squared errors (MSE) for each evaluated application. The MSE is computed for normalized pixels (range [0-1]). The average MSE over all perturbed samples is reported for each attack.

Application	Attack	$\epsilon$	n <sub>iters</sub>	MSE
MNIST	FSG	{0.001, 0.002, 0.005, 0.01, 0.02, 0.05, 0.1}	1	4.3e-3
	JSMA	0.1	{1.5,10,20,50}	6.4e-4
	Deepfool	0.05	{1.5,10,20,50}	1.85e-3
CIFAR	FSG	{0.001, 0.002, 0.005, 0.01}	1	3.7e-5
	JSMA	0.1	{1.5,10,20,50}	6.6e-5
	Deepfool	0.05	{1.5,10,20,50}	9.2e-5
Imagenet	FSG	{0.001, 0.002, 0.005, 0.01, 0.02}	1	1.7e-4
	JSMA	0.1	{1.5,10,20,50}	6.2e-5
	Deepfool	1	{1.5,10,20,50}	7.2e-6

challenging for both human observers and automated agents.

**CuRTAIL Input Dictionaries.** We evaluate the impact of CuRTAIL input dictionaries (Section V-B2) for each application and attack scenario. The denoising module learns pertinent dictionaries for non-overlapping patches of pixels for each data set. Specifically, we learn dictionaries of  $K_{max} = 225$  columns for each class within the datasets. The patch size is set to  $7 \times 7$ ,  $8 \times 8$ , and  $16 \times 16$  for the MNIST, CIFAR-10, and Imagenet datasets, respectively.

We define the *false positive* rate as the ratio of legitimate test samples that are mistaken for adversarial samples by CuRTAIL. The *true positive* rate is defined as the ratio of adversarial samples detected by CuRTAIL. Figure 12 depicts the false positive and true positive rates of CuRTAIL denoising module for different numbers of non-zeros,  $K$ , in the pertinent sparse representations. Our experiments show that increasing  $K$  results in lower true positive and false positive rates. To discuss the enabler of this trade-off between false positives and true positives, we show an example target sample along with the corresponding perturbed adversarial sample and denoised images in Figure 13. As can be seen, employing a higher  $K$  reduces the effect of image denoising and allows the perturbed pixels to contribute to deceiving the victim DL model, whereas a lower  $K$  will remove such perturbations from the adversarial samples. On the other hand, small values of  $K$  can result in poorly reconstructed images which can cause the framework to infer legitimate samples as infected inputs, increasing the



Fig. 13: An example adversarial sample and its corresponding denoised images. The original image was drawn from the Imagenet dataset and the JSMA attack was used to craft the adversarial sample.

false positive rate. The reconstruction parameter  $K$  can be tuned based on the target application.

**CuRTAIL Latent Dictionaries.** For each application, we train a complementary neural network (see Section V-B1) with the checkpoint placed at the second-to-last layer. More specifically, we initialize the weights of the complementary network using those of the victim model, then retrain the defender model by adding the extra term to the loss function with parameter  $\gamma$  set to 0.01 for all applications (see Equation 11). For each application, we retrain the model with the same optimizer used for training the victim model, and we set the learning rate of the optimizer to  $\frac{1}{10}$  of that of the victim model. Once the defender modules are trained, the low dimensional PCA features and the corresponding Gaussian PDF estimators are constructed as discussed in Section V-B1. We use the PDF models with different security parameters to detect adversarial samples. Figure 14 demonstrates an example of the adversarial confusion matrices for victim neural networks and CuRTAIL *latent dictionaries* output with a security parameter as low as only 1%. The confusion matrices are computed for the FSG attack (Section III). As shown, CuRTAIL effectively removes/detects adversarial inputs by looking into minimally overlapping statistical latent dictionaries learned to cover unexplored data sub-spaces in the victim DL network. The remaining adversarial samples that are not detected in this experiment are crafted from legitimate samples that are inherently hard to classify even by a human observer due to the closeness of decision boundaries corresponding to such classes. For instance, in the MNIST application, such adversarial samples mostly belong to class 5 that is misclassified to class 3 or class 4 misclassified as 9. Such misclassifications are indeed the model approximation error which is well-understood to the statistical nature of the models. Figure 16 illustrates several of

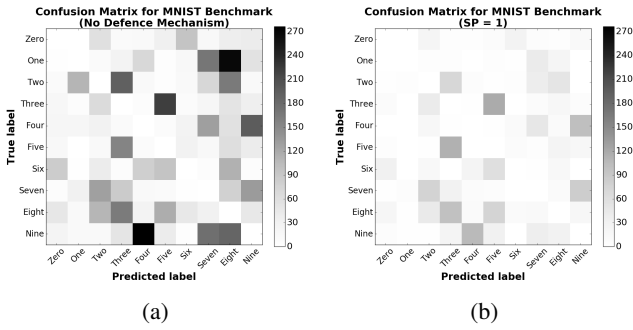


Fig. 14: Example adversarial confusion matrices for the MNIST benchmark. (a) Confusion matrix without a defense mechanism. (b) Confusion matrix after employing latent dictionaries with a security parameter of (1%).

these examples in each application. Note that the remaining adversarial samples in this experiment can be effectively filtered out in CuRTAIL framework by considering a higher security parameter (e.g.,  $SP = 5\%$ ). The higher detection rate may come at the cost of adding several false positives to the detection process as we discuss in the rest of this section.

CuRTAIL jointly considers the input and latent dictionaries to detect adversarial samples. In particular, we treat an input as an adversarial sample if either of the latent or input dictionaries raise an alarm signal. To evaluate the joint decision metric for each application and attack scenario, we evaluate the false positive and true positive rates and present the pertinent Receiver Operating Characteristic (ROC) curves in Figure 15. The ROC curves are established as follows: We change the security parameter  $SP$  for the detector modules (Section V-B1) in the range of [0.001-100] and evaluate the FP and TP rates for each security parameter to obtain the dashed blue curves in Figure 15. Next, we fix the denoising parameter  $K$  to 4, 32, and 16 for the MNIST, CIFAR-10, and Imagenet datasets, respectively. We repeat the experiments by changing the security parameter  $SP$  and observing the ROC curve but this time we also adopt the decision function of the denoiser module, which results in the solid green ROC curves in Figure 15.

The diagonal line indicates the trajectory that would be obtained by random prediction. This figure precisely outlines the disjoint impact of latent and input dictionaries for each adversary attack. As can be seen from the ROC curves, high detection rate can be achieved while accepting a small false positive rate. For instance, for the MNIST dataset, CuRTAIL can detect around 90% of the adversarial samples with a FP rate less than 5%. Note that both the security parameter  $SP$  and the denoising parameter  $K$  can be dynamically tuned after the initial PDFs and input dictionaries are established; therefore, CuRTAIL can be adapted to various applications which require different levels of security. Last but not the least, the effect of input dictionaries in CuRTAIL depends on the amount of noise added to adversarial samples. As we discussed earlier, we have configured the attack algorithms in a way that the evaluated adversarial samples include a significantly small amount of noise (see Table IV), thus, the

contribution of the input dictionary might not be as significant as the latent dictionary in our experiments. Nevertheless, the input dictionaries can provide an effective tool for detecting adversarial samples with higher amounts of additive noise.

## VII. RELATED WORK

Securing machine learning models against adversarial samples is an important step towards building intelligent and autonomous systems that are reliable and trustworthy [1]. The existence of adversarial samples and their severe impact on the integrity of autonomous systems have been shown in the literature for both shallow [14], [40], [41], [42], [43] and deep [11], [12], [13], [44] learning models. Depending on the adversary goals, the adversarial attacks are performed either in the training process of a model (e.g., [45], [46]) or during the execution time where an already trained model is leveraged for data inference (e.g., [12], [40]).

Prior works on adversarial deep learning have been mainly focused on devising novel attacks for DL execution time. A comprehensive discussion of existing DL attacks has been presented in Section III. In this paper, we consider a white-box threat model where the adversary knows everything about the DL model and its parameters. This is the strongest adversary that might appear in real-world applications. To the best of our knowledge, CuRTAIL is the first framework that provides an end-to-end methodology for effectively thwarting adversarial samples crafted attackers with full knowledge about the target DL model.

Several research efforts have been made at devising DL models that are resilient to adversarial perturbations. Authors in [12] show that the use of radial basis activation functions can result in DL models with better generalization properties. Leveraging such activation functions require fundamental modification to the current DL architectures making this approach irrelevant to existing learning models. Another viable countermeasure proposed in the literature is the use of denoising auto-encoders to capture data perturbation created by adversaries. The resulting stacked architecture is no more robust against white-box adversarial attacks as shown in [16]. The authors in [16] propose a new architecture called Deep Contractive Networks by imposing a layer-wise penalty based on the network's Jacobian matrix. Although this penalty can potentially reduce the vulnerability of DL model against adversarial perturbations, it imposes a strict limitation to the learning capacity of deep contractive networks compared to the conventional DL architecture.

Network pruning and distillation are other defense mechanisms proposed in the literature to train more robust DL networks by smoothing the gradient space in the output layer and removing unnecessary connections in the DL topology [21]. Recent follow-up papers (e.g., [22]), however, have demonstrated that even the distilled networks can be easily compromised by computing the adversarial gradient with respect to the intermediate layers of the DL model. The key enabler of such attacks is the fact that all the existing works rely on a single model to perform.

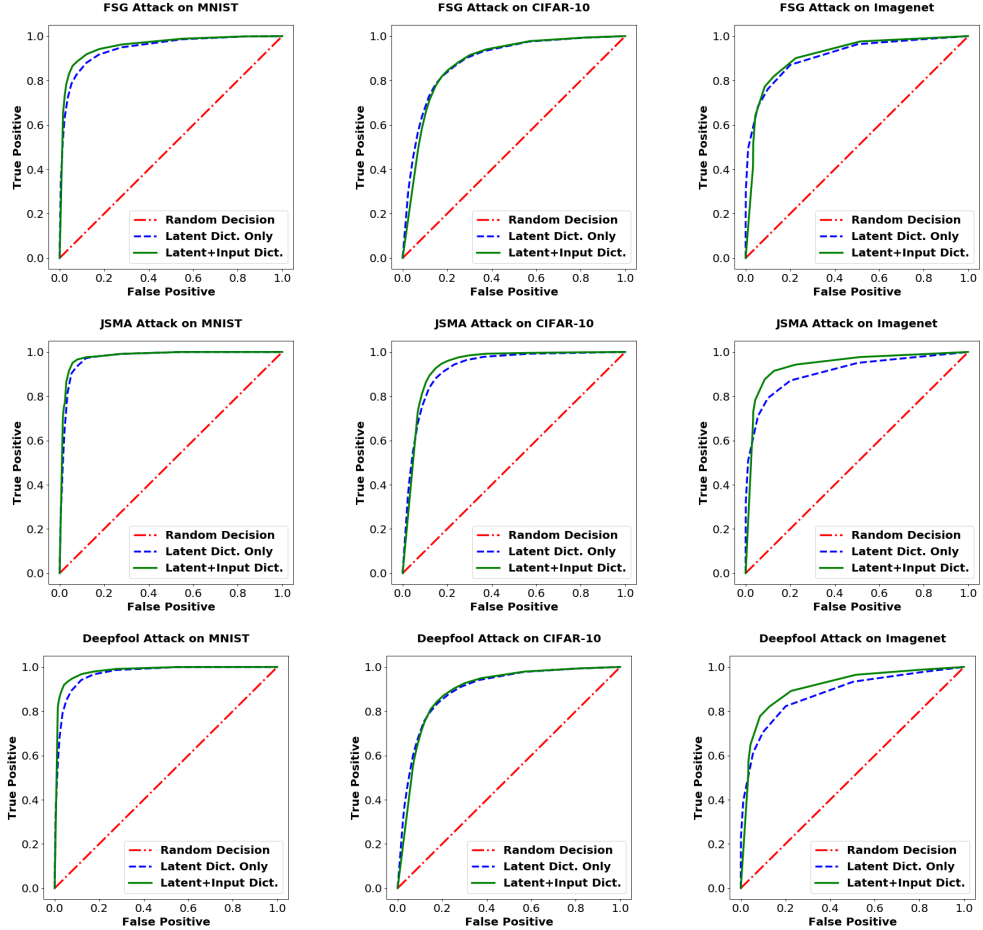


Fig. 15: true positive versus false positive rates in each application. The top, middle, and bottom rows corresponds to adversarial samples generated by FSG [12], JSMA [13], and Deepfool [27] attacks, respectively.

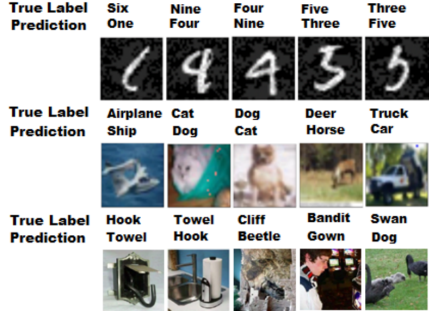


Fig. 16: Example adversarial samples for which accurate detection is hard due to the closeness of decision boundaries for the corresponding classes.

To the best of our knowledge, CuRTAIL is the first to introduce modular redundancy as a robust defense mechanism to defeat DL adversarial samples with no drop in the accuracy or learning capability of the main deep neural network. This is because CuRTAIL defensive redundancy modules are trained to work in parallel to the victim DL model, thus, they do not affect the decision boundaries and the accuracy of the main classifier. As corroborated in Section VI, CuRTAIL is capable of accurate detection of the state-of-the-art attack

models including fast-sign-gradient [12], Jacobian Saliency Map Attack [13], and Deepfool [27]. We emphasize that the MRR methodology provides a rather generic approach that can be adapted/modified against potential new attacks that might be proposed in future.

## VIII. CONCLUSION

This paper proposes CuRTAIL, a novel end-to-end framework for characterizing and thwarting adversarial DL space. We propose a set of novel quantitative measurements to assess and compare the vulnerability of various DL topologies. CuRTAIL introduces the concept of Modular Robust Redundancy as a viable countermeasure to maximally cover the space unexplored by the victim DL mode thus reducing the risk of integrity attacks. The MRR methodology explicitly characterizes statistical properties of the features within different layers of the neural network by learning a set of complementary dictionaries and corresponding probability density functions. CuRTAIL effectiveness is evaluated against the state-of-the-art attack models including fast-sign-gradient, Jacobian Saliency Map Attack, and Deepfool. Proof-of-concept experiments for analyzing various data collections including MNIST, CIFAR10, and ImageNet datasets corroborate the proposed methodology.

orate successful detection of adversarial samples with small false-positive rates. Our proposed framework is devised with an accompanying automated API to ensure ease of use for deployment of an arbitrarily DL application.

## REFERENCES

- [1] P. McDaniel, N. Papernot, and Z. B. Celik, "Machine learning in adversarial settings," *IEEE Security & Privacy*, vol. 14, no. 3, pp. 68–72, 2016.
- [2] Y. LeCun, Y. Bengio, and G. Hinton, "Deep learning," *Nature*, vol. 521, no. 7553, pp. 436–444, 2015.
- [3] L. Deng, D. Yu *et al.*, "Deep learning: methods and applications," *Foundations and Trends® in Signal Processing*, vol. 7, no. 3–4, pp. 197–387, 2014.
- [4] G. Hinton, L. Deng, D. Yu, G. E. Dahl, A.-r. Mohamed, N. Jaitly, A. Senior, V. Vanhoucke, P. Nguyen, T. N. Sainath *et al.*, "Deep neural networks for acoustic modeling in speech recognition: The shared views of four research groups," *IEEE Signal Processing Magazine*, vol. 29, no. 6, pp. 82–97, 2012.
- [5] G. E. Dahl, D. Yu, L. Deng, and A. Acero, "Context-dependent pre-trained deep neural networks for large-vocabulary speech recognition," *IEEE Transactions on Audio, Speech, and Language Processing*, vol. 20, no. 1, pp. 30–42, 2012.
- [6] A. Krizhevsky, I. Sutskever, and G. E. Hinton, "Imagenet classification with deep convolutional neural networks," pp. 1097–1105, 2012.
- [7] Y. Taigman, M. Yang, M. Ranzato, and L. Wolf, "Deepface: Closing the gap to human-level performance in face verification," pp. 1701–1708, 2014.
- [8] E. Knorr, "How paypal beats the bad guys with machine learning," 2015.
- [9] G. E. Dahl, J. W. Stokes, L. Deng, and D. Yu, "Large-scale malware classification using random projections and neural networks," pp. 3422–3426, 2013.
- [10] Z. Yuan, Y. Lu, Z. Wang, and Y. Xue, "Droid-sec: deep learning in android malware detection," vol. 44, no. 4, pp. 371–372, 2014.
- [11] C. Szegedy, W. Zaremba, I. Sutskever, J. Bruna, D. Erhan, I. Goodfellow, and R. Fergus, "Intriguing properties of neural networks," *arXiv preprint arXiv:1312.6199*, 2013.
- [12] I. J. Goodfellow, J. Shlens, and C. Szegedy, "Explaining and harnessing adversarial examples," *arXiv preprint arXiv:1412.6572*, 2014.
- [13] N. Papernot, P. McDaniel, S. Jha, M. Fredrikson, Z. B. Celik, and A. Swami, "The limitations of deep learning in adversarial settings," pp. 372–387, 2016.
- [14] L. Huang, A. D. Joseph, B. Nelson, B. I. Rubinstein, and J. Tygar, "Adversarial machine learning," pp. 43–58, 2011.
- [15] M. Barreno, B. Nelson, R. Sears, A. D. Joseph, and J. D. Tygar, "Can machine learning be secure?" pp. 16–25, 2006.
- [16] S. Gu and L. Rigazio, "Towards deep neural network architectures robust to adversarial examples," *arXiv preprint arXiv:1412.5068*, 2014.
- [17] J. Jin, A. Dundar, and E. Culurciello, "Robust convolutional neural networks under adversarial noise," *arXiv preprint arXiv:1511.06306*, 2015.
- [18] R. Huang, B. Xu, D. Schuurmans, and C. Szepesvári, "Learning with a strong adversary," *arXiv preprint arXiv:1511.03034*, 2015.
- [19] U. Shaham, Y. Yamada, and S. Negahban, "Understanding adversarial training: Increasing local stability of neural nets through robust optimization," *arXiv preprint arXiv:1511.05432*, 2015.
- [20] S. Zheng, Y. Song, T. Leung, and I. Goodfellow, "Improving the robustness of deep neural networks via stability training," pp. 4480–4488, 2016.
- [21] N. Papernot, P. McDaniel, X. Wu, S. Jha, and A. Swami, "Distillation as a defense to adversarial perturbations against deep neural networks," pp. 582–597, 2016.
- [22] N. Carlini and D. Wagner, "Defensive distillation is not robust to adversarial examples," *arXiv preprint*, 2016.
- [23] J. Mairal, J. Ponce, G. Sapiro, A. Zisserman, and F. R. Bach, "Supervised dictionary learning," pp. 1033–1040, 2009.
- [24] Y. LeCun, C. Cortes, and C. J. Burges, "The mnist database of handwritten digits," 1998.
- [25] A. Krizhevsky and G. Hinton, "Learning multiple layers of features from tiny images," 2009.
- [26] J. Deng, W. Dong, R. Socher, L.-J. Li, K. Li, and L. Fei-Fei, "ImageNet: A Large-Scale Hierarchical Image Database," 2009.
- [27] S.-M. Moosavi-Dezfooli, A. Fawzi, and P. Frossard, "Deepfool: a simple and accurate method to fool deep neural networks," in *Proceedings of the IEEE Conference on Computer Vision and Pattern Recognition*, 2016, pp. 2574–2582.
- [28] L. Bottou, "Large-scale machine learning with stochastic gradient descent," pp. 177–186, 2010.
- [29] N. Papernot, P. McDaniel, I. Goodfellow, S. Jha, Z. B. Celik, and A. Swami, "Practical black-box attacks against deep learning systems using adversarial examples," *arXiv preprint arXiv:1602.02697*, 2016.
- [30] B. Wang, J. Gao, and Y. Qi, "A theoretical framework for robustness of (deep) classifiers under adversarial noise," *arXiv preprint arXiv:1612.00334*, 2016.
- [31] Y. Wen, K. Zhang, Z. Li, and Y. Qiao, "A discriminative feature learning approach for deep face recognition," pp. 499–515, 2016.
- [32] Y. LeCun, L. Bottou, Y. Bengio, and P. Haffner, "Gradient-based learning applied to document recognition," *Proceedings of the IEEE*, vol. 86, no. 11, pp. 2278–2324, 1998.
- [33] I. Jolliffe, *Principal component analysis*. Wiley Online Library, 2002.
- [34] A. Mirhoseini, E. L. Dyer, E. Songhori, R. G. Baraniuk, F. Koushanfar *et al.*, "Rankmap: A platform-aware framework for distributed learning from dense datasets," *arXiv preprint arXiv:1503.08169*, 2015.
- [35] B. D. Rouhani, A. Mirhoseini, and F. Koushanfar, "Delight: Adding energy dimension to deep neural networks," pp. 112–117, 2016.
- [36] J. Tropp, A. C. Gilbert *et al.*, "Signal recovery from random measurements via orthogonal matching pursuit," *IEEE Transactions on Information Theory*, vol. 53, no. 12, pp. 4655–4666, 2007.
- [37] D. Ciregan, U. Meier, and J. Schmidhuber, "Multi-column deep neural networks for image classification," pp. 3642–3649, 2012.
- [38] N. Srivastava, G. E. Hinton, A. Krizhevsky, I. Sutskever, and R. Salakhutdinov, "Dropout: a simple way to prevent neural networks from overfitting," *Journal of Machine Learning Research (JMLR)*, vol. 15, no. 1, pp. 1929–1958, 2014.
- [39] M. Abadi, A. Agarwal, P. Barham, E. Brevdo, Z. Chen, C. Citro, G. S. Corrado, A. Davis, J. Dean, M. Devin *et al.*, "Tensorflow: Large-scale machine learning on heterogeneous distributed systems," *arXiv preprint arXiv:1603.04467*, 2016.
- [40] B. Biggio, I. Corona, D. Maiorca, B. Nelson, N. Šrndić, P. Laskov, G. Giacinto, and F. Roli, "Evasion attacks against machine learning at test time," pp. 387–402, 2013.
- [41] B. Biggio, G. Fumera, and F. Roli, "Pattern recognition systems under attack: Design issues and research challenges," *International Journal of Pattern Recognition and Artificial Intelligence*, vol. 28, no. 07, p. 1460002, 2014.
- [42] A. Anjos and S. Marcel, "Counter-measures to photo attacks in face recognition: a public database and a baseline," pp. 1–7, 2011.
- [43] P. Fogla and W. Lee, "Evading network anomaly detection systems: formal reasoning and practical techniques," pp. 59–68, 2006.
- [44] J. Kos, I. Fischer, and D. Song, "Adversarial examples for generative models," *arXiv preprint arXiv:1702.06832*, 2017.
- [45] B. Biggio, B. Nelson, and P. Laskov, "Support vector machines under adversarial label noise," *ACML*, vol. 20, pp. 97–112, 2011.
- [46] ———, "Poisoning attacks against support vector machines," *arXiv preprint arXiv:1206.6389*, 2012.